Electronic Supplementary Material (ESI) for Journal of Materials Chemistry A
This journal is © The Royal Society of Chemistry 2013

Supporting Information

Hydrothermal Synthesis of α-MnO_2 and β-MnO_2 Nanorods as High Capacity Cathode Materials for Sodium Ion Batteries

Dawei Su,[a] Hyo-Jun Ahn,[b] and Guoxiu Wang[a,b,]*

[a]Centre for Clean Energy Technology, School of Chemistry and Forensic Science, University of Technology, Sydney, Sydney, NSW 2007, Australia

[b]School of Materials Science and Engineering, Gyeongsang National University, 900 Gazwa-dong, Jinju, Gyeongnam 660-701, Republic of Korea

[*] Prof. G. X. Wang

E-mail: Guoxiu.Wang@uts.edu.au

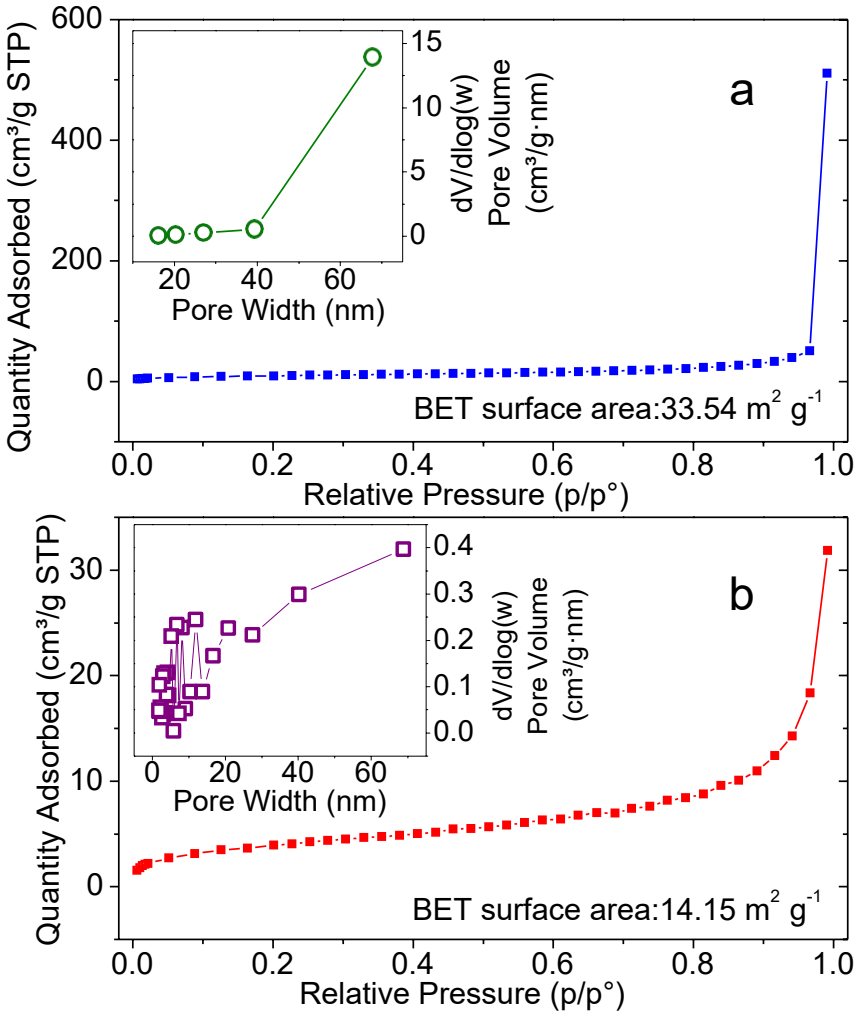

Fig. S1. N_2 absorption isotherms of α-MnO_2 nanorods (a) and β-MnO_2 nanorods (b). Insets are their corresponding pore size distributions derived from absorption hysteresis of Brunauer-Emmett-Teller (BET) surface area measurement.

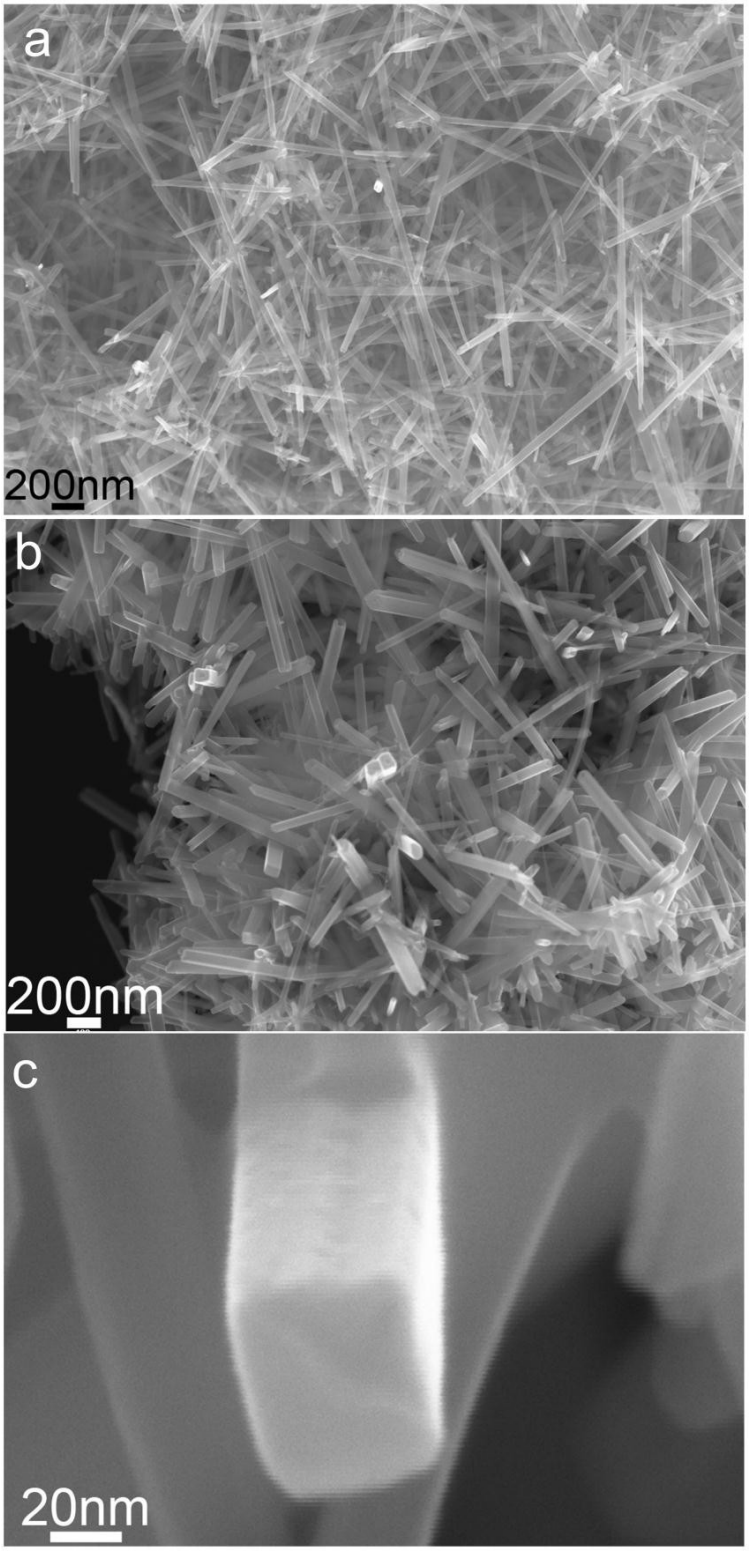

Fig. S2. Low magnification (a and b) and high magnification (c) FESEM images of α-MnO_2 nanorods.

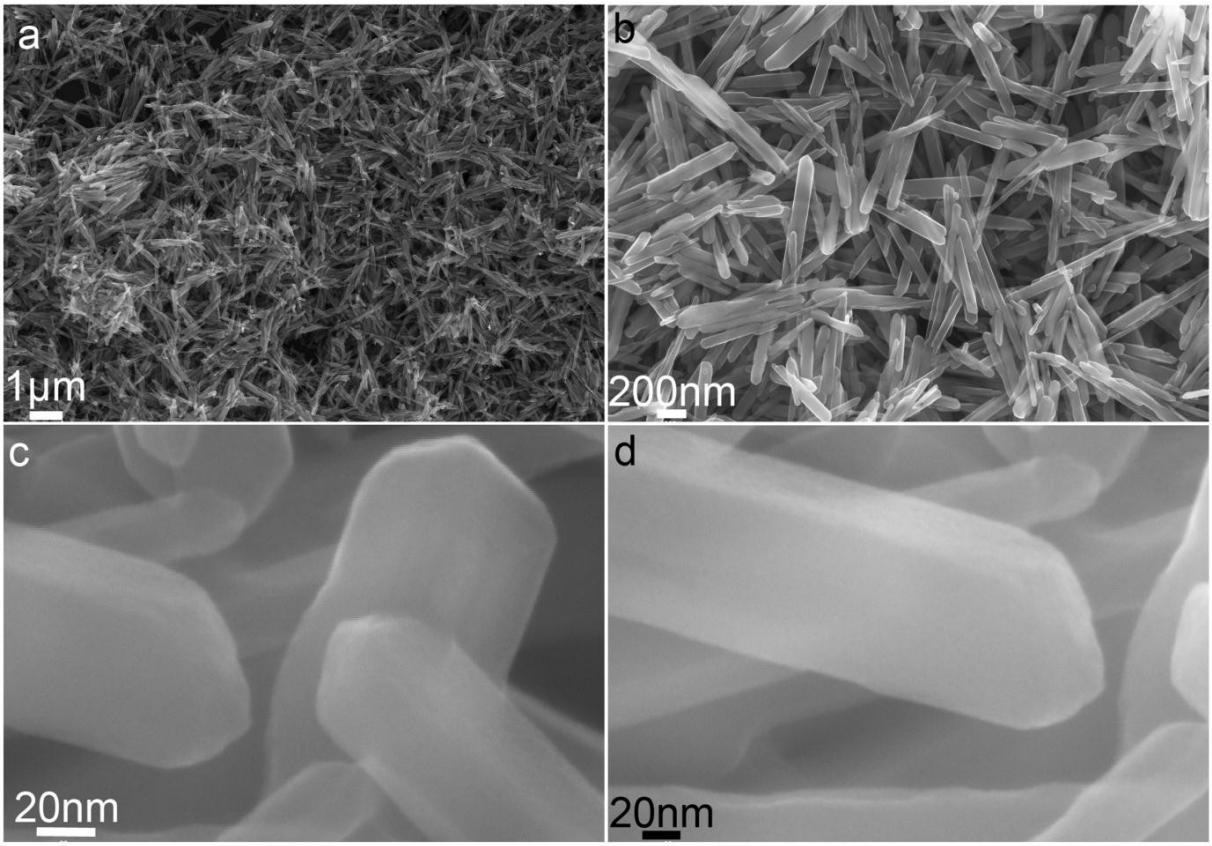

Fig. S3. Low magnification (a), medial magnification (b), and high magnification (c and d) FESEM images of β-MnO_2 nanorods.

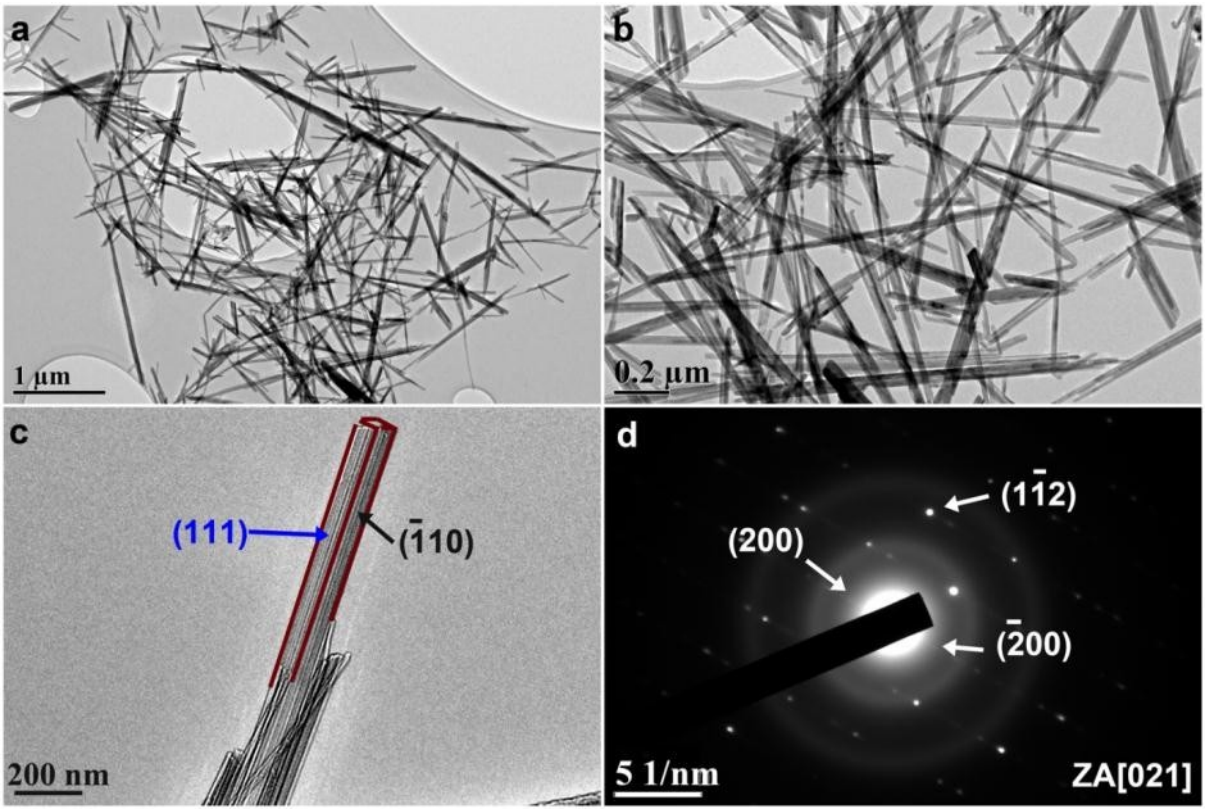

Fig. S4. Low (a) and medial (b) magnification TEM images of α-MnO_2 nanorods. c. A single α-MnO_2 nanorod with the [021] projected direction, in which the (111) and $\bar{1}$10) crystal planes are marked. And d is its corresponding SAED patterns which can be indexed along the [021] zone axis of tetragonal α-MnO_2.

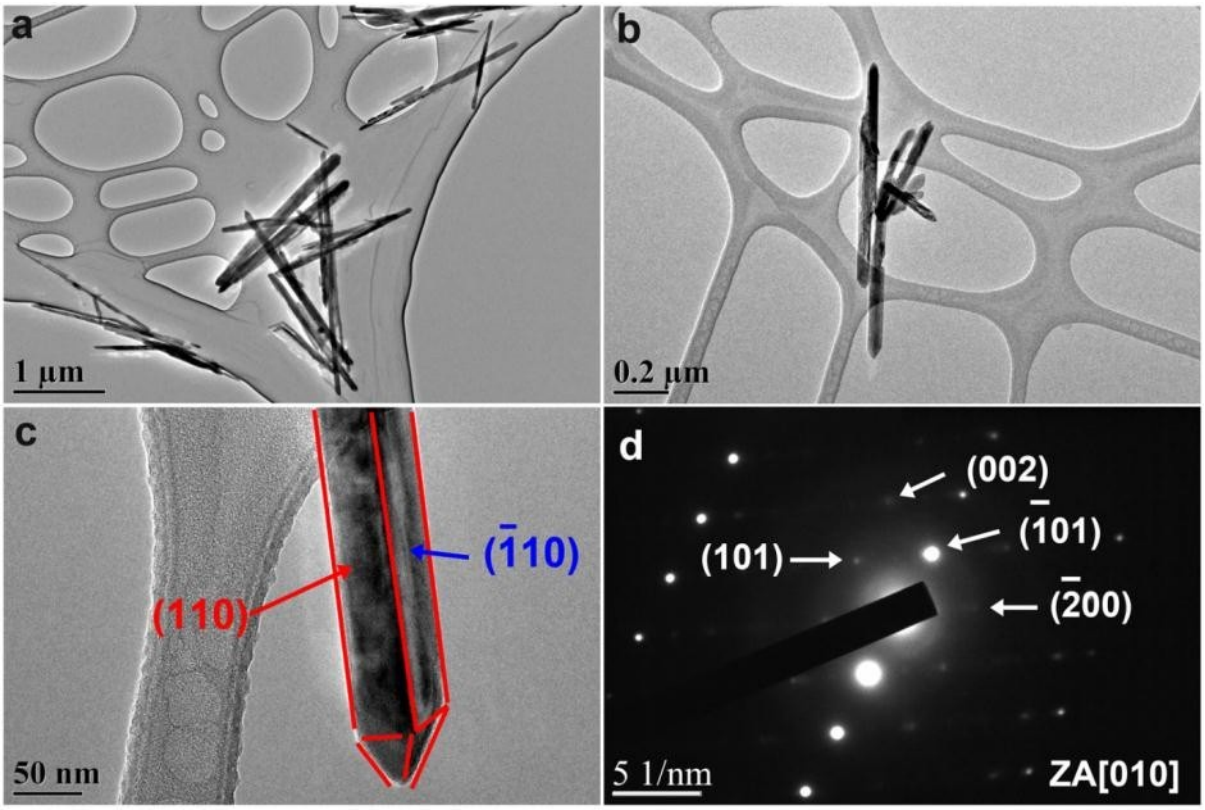

Fig. S5. Low (a) and medial (b) magnification TEM images of β-MnO_2 nanorods. c. A single β-MnO_2 nanorod with the [010] projected direction in which the (110) and $\bar{1}$10) crystal planes are marked. And d is its corresponding SAED patterns which can be indexed along the [010] zone axis of tetragonal β-MnO_2.

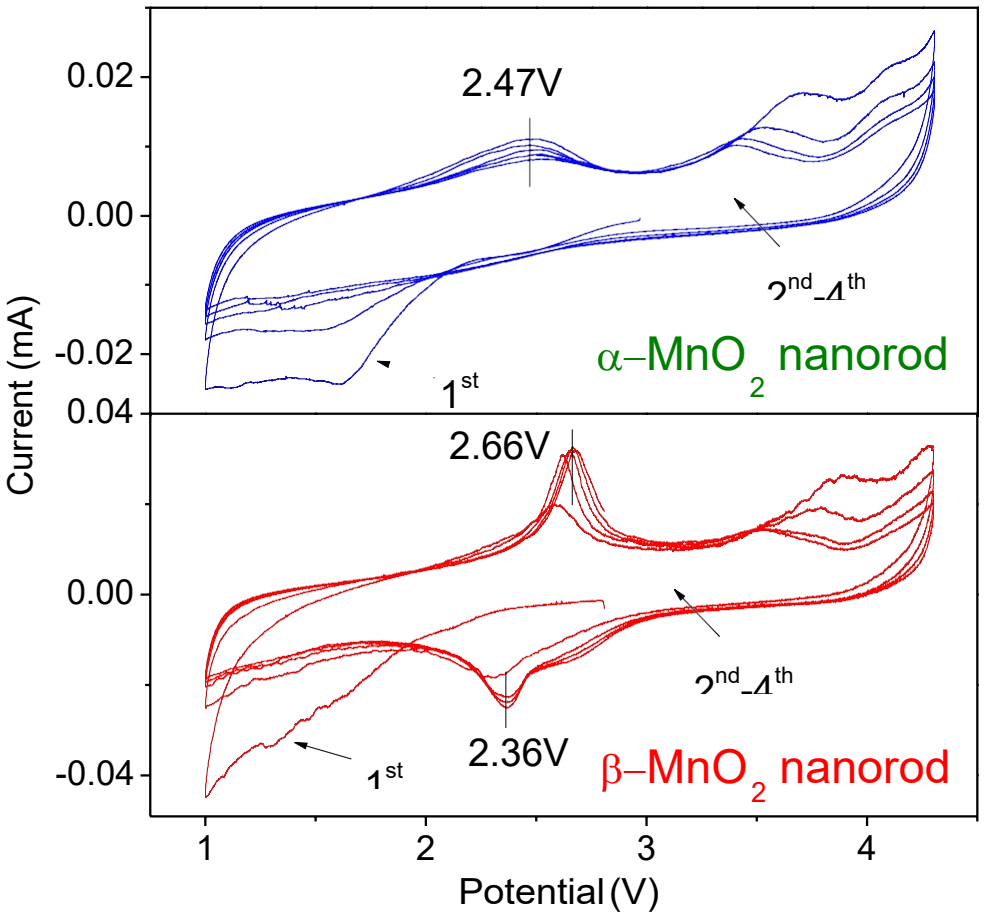

Fig. S6. The CV curves of the α-MnO_2 nanorods and β-MnO_2 nanorods as cathodes in sodium ion cells.

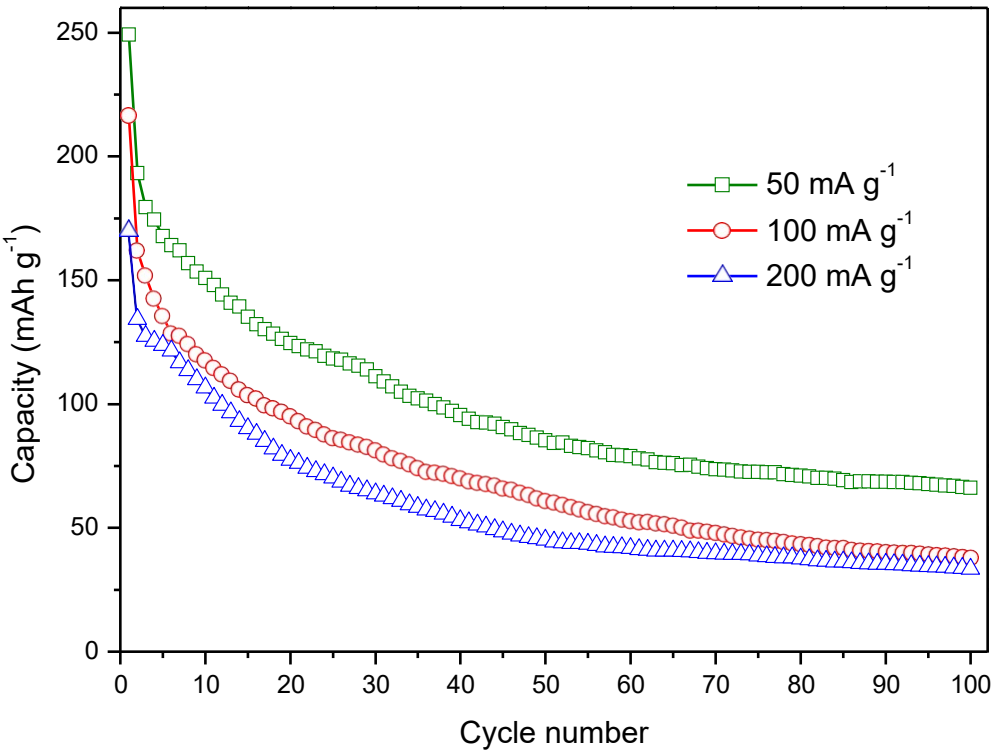

Fig. S7. Discharge capacity vs. cycle number of α-MnO_2 nanorods at different current densities of 50, 100, and 200 mA g^{-1}.

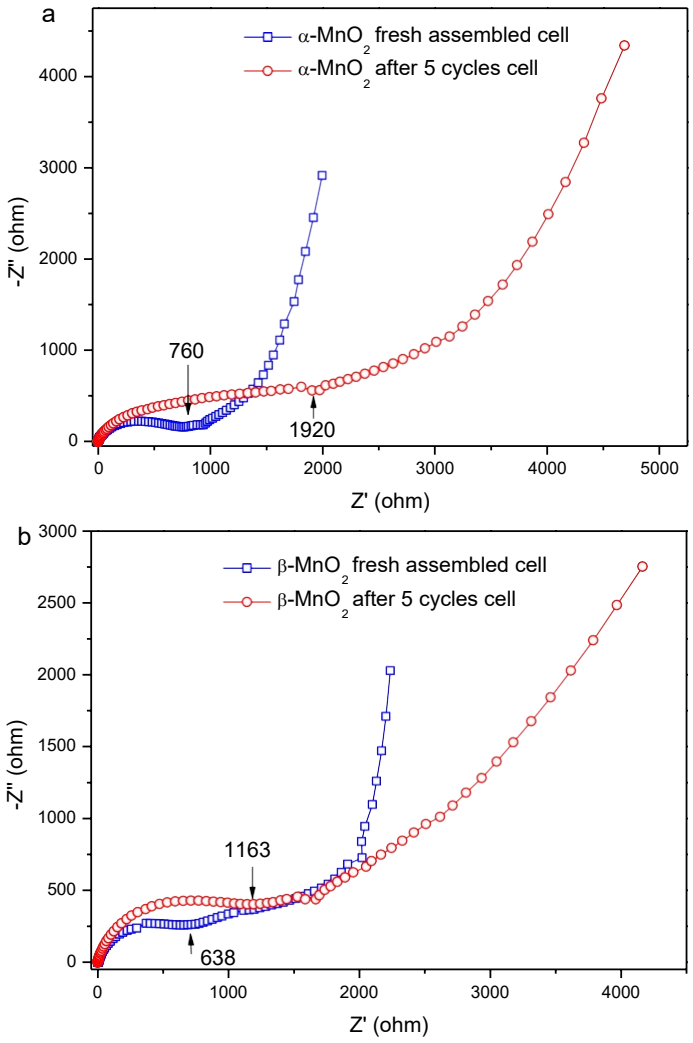

Fig. S8 The Nyquist plots of α-MnO_2 nanorods (a) and β-MnO_2 nanorods (b) in freshly assembled test cell and after 5 cycles in the frequency range between 100 kHz and 10 mHz at room temperature.

Density Function Theory (DFT) Calculation Method

DFT calculations were performed using the Vienna Ab initio Simulation Package[1-4] based on the Generalized Gradient Approximation (GGA)[5] with Hubbard U (U=5.2 eV for the transition metal Mn)[6,7] corrections (GGA+U).[8] The projector augmented wave potentials[9] with the cutoff energy of 450 eV applied. Relaxation simulations were performed for ionic positions, unit cell shape, and unit cell size. For Mn, the 3p, 3d, and 4s states were treated as valence states. For O, the 2s and 2p states were treated as valence states. The conjugate gradient scheme is used to optimize the atom coordinates until the force is less than 0.01 eV $Å^{-1}$.

For the bulk $P4_2/mnm$ β-MnO_2 crystal and I4/m α-MnO_2, 1 × 1 × 1 unit cells were used for the crystal structure relaxation. The Γ-centered Monkhorst-Pack[10] K-points 6 × 6 × 10 and 3 × 3 × 5 were used for β-MnO_2 and α-MnO_2 crystals, respectively. After getting the relaxed bulk β-MnO_2 and α-MnO_2 crystal structures, the {001} and {110} crystal planes of β-MnO_2 and {001} and {100} crystal planes of α-MnO_2 were cleaved correspondingly. At least five layers of atoms were obtained for each of the facets. A vacuum level of 15 Å for the layer structures was built. The D3 correction was applied for all the layer structure calculations to consider the Van der Walls effect. The K-points of 6 × 6 × 1, 8 × 4 × 1, 2 × 2 × 1, and 2 × 8 × 1were used for {001} and {110} crystal planes of β-MnO_2 and {001} and {100} crystal planes of α-MnO_2, respectively. The relaxed structures of the facets absorbed with the Na^+ ions can be found after the References session below.

To calculate the Na^+ ions binding energy, the energy of 1 × 1 × 1 unit cell of body-centered cubic Sodium crystal was calculated. Then the single Na atom energy (E_{Na}) was obtained by dividing the sodium number of the unit cell. The binding energies (E_b) were calculated by:

$$E_b = (E_{facets\ absorbed\ Na^+\ ions} - E_{facets} - nE_{Na})/n$$

Where, $E_{facets\ absorbed\ Na^+\ ions}$, E_{facets}, *and* n are the energy of facets absorbed with Na^+ ions, the energy of the facets and the absorbed Na^+ ions number, respectively.

DFT Results and Discussion

Here, we further applied the DFT calculations to analyse the sodium ions' interaction with different facets of the β-MnO_2 ({001} and {110}) and α-MnO_2 ({001} and {100}). The detailed calculation method and relaxed crystal structures were supplied in the last session of this response letter.

As shown in **Figs. S9 a and b**, after the lattice and atoms relaxation calculations on {001} facets of β-MnO_2, all the Na^+ ions stabilize on the 8h Wyckoff position ($P4_2$/~~mum~~ mnm space group), that are above the bottleneck (window) of the [1 × 1] tunnel of β-MnO_2. Na^+ ions are two-fold coordinated with the oxygen ligands of the MnO_6 octahedron with the 2.262 Å bond length as marked in the side view of the relaxed {001} facets of β-MnO_2 (**Fig. S9b**). While for the I4/m space group α-MnO_2, after the lattice and atoms relaxation calculations (**Figs. S9 c and d**), in each unit cell, two Na^+ ions stabilize on the 8g Wyckoff position, that is above the bottleneck (window) of the [1 × 1] tunnel of α-MnO_2, that are two-fold coordinated with the oxygen ligands of the MnO_6 octahedron with the 2.245 Å bond length. One Na^+ ion localizes on the 2a Wyckoff position (the cavity centre of the [2 × 2] tunnel), eight-fold coordinated with the oxygen ligands of the MnO_6 octahedron with an average ~2.61 Å bond length (form the cube shortened along c axis geometry) as marked in the side view of the relaxed {001} facets of α-MnO_2 (**Fig. S9c**). There is one more Na^+ ion occupying the 2b Wyckoff position, forming a four-fold coordination geometry with an average ~2.61 Å bond length.

Figs. S10 a and b show the lattice and atoms relaxed oxygen termination {110} facets of β-MnO_2 (oxygen termination {110} facets of β-MnO_2 have 131 meV lower free energy compared with the manganese terminated facets). All the Na^+ ions two-fold coordinate with the 4f Wyckoff position oxygen, forming the 2.192 Å bond length as shown in **Fig. S10b**. While for the oxygen terminated {100} facets of α-MnO_2 (**Figs. S10 c and d,** oxygen termination {100} facets of α-MnO_2 have 954 meV lower free energy compared with the manganese terminated facets), in each unit cell, one Na^+ ion four-fold coordinates with 8h Wyckoff position oxygens (with two 2.168 Å bond lengths and two 2.587 Å bond lengths), that is inserted within the half [1 × 1] tunnel. Another Na^+ ion inserts the half [2 × 2] tunnels, forming the V coordination geometry with 8h Wyckoff position oxygens (with four ~2.32 Å bond lengths and one 2.665 Å bond length) as shown in **Figs. S10 c and d**.

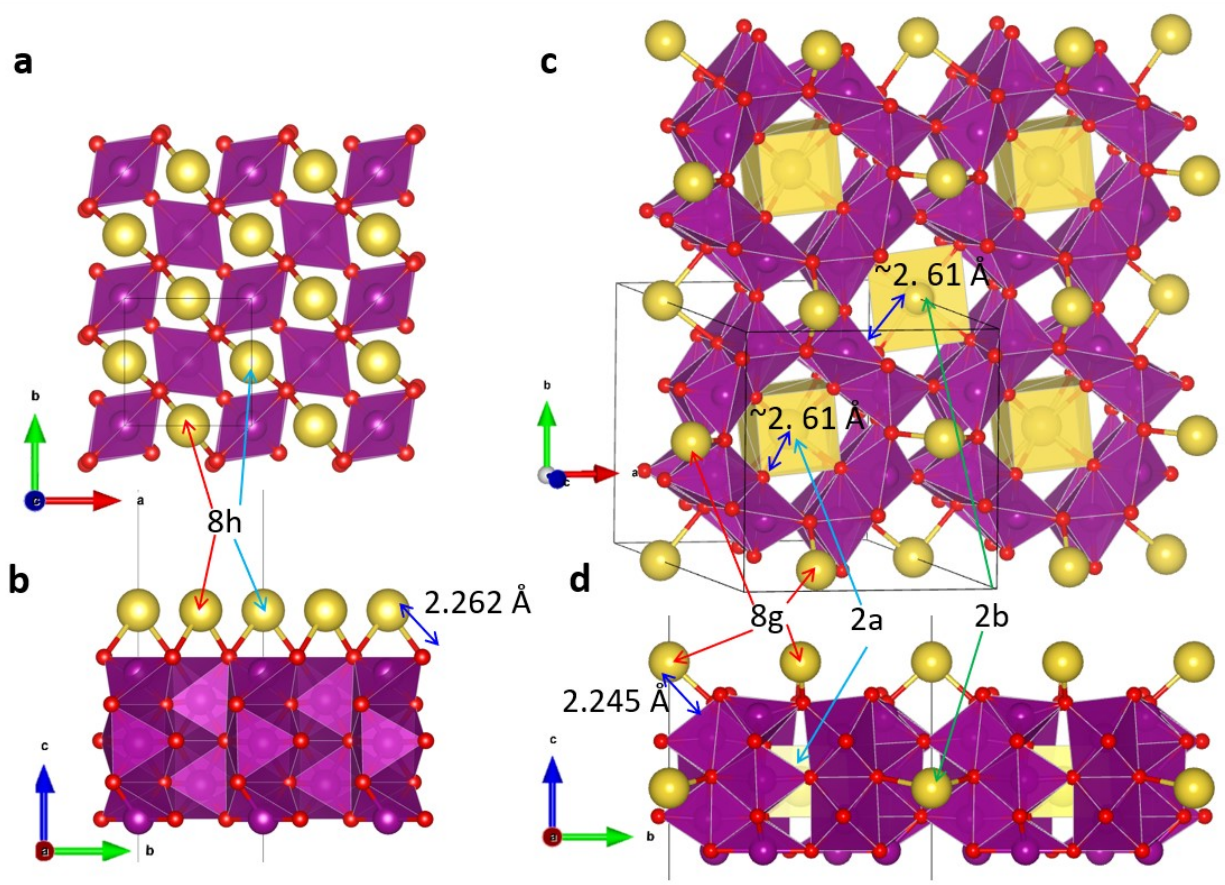

Fig. S9. a and b. Top (a) and side (b) views of the relaxed {001} facets of β-MnO_2 absorbed with the Na^+ ions. c and d. Top (c) and side (d) views of the relaxed {001} α -MnO_2 absorbed with the Na^+ ions. Yellow, purple, and red spheres are Na, Mn, and O atoms, respectively. Red, green, and blue coloured arrows represent the a, b, and c axes, respectively. Plotted by the VESTA.[11]

The Na^+ ion binding energy on the relaxed {001} and {110} facets of β-MnO_2 are -0.709 and -0.976 eV, respectively, as shown in **Table S1**. They are smaller than the values of relaxed {001} and {100} facets of α-MnO_2 (-2.575 and -1.875 eV, respectively), which could be ascribed to the lower coordination number (two-fold) of Na^+ ions absorbed above the bottleneck of β-MnO_2 {001} facets [1 × 1] tunnel and coordinated with the 4f Wyckoff position oxygen of β-MnO_2 {110} facets. With the large cavity [2 × 2] tunnel, α-MnO_2 could accommodate the Na^+ ions to form eight-fold coordination NaO_8 geometry (2a site) and spare planer NaO_4 geometry (2b site) through the {001} facets, resulting in the much higher binding energy with Na^+ ions.

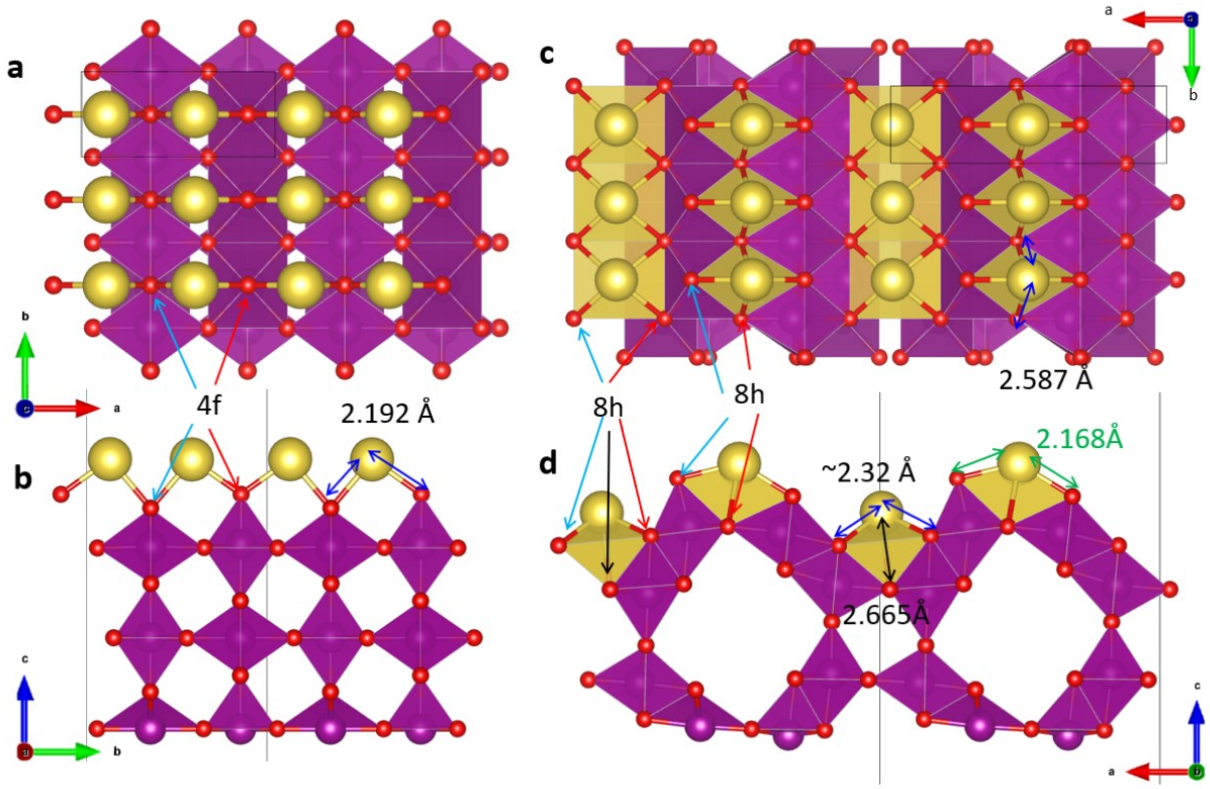

Fig. S10. a and b. Top (a) and side (b) views of the relaxed {110} facets of β-MnO_2 absorbed with the Na^+ ions. c and d. Top (c) and side (d) views of the relaxed {100} α-MnO_2 absorbed with the Na^+ ions. Yellow, purple, and red spheres are Na, Mn, and O atoms, respectively. Red, green, and blue coloured arrows represent the a, b, and c axes, respectively. Plotted by the VESTA.[11]

Table S1. Binding energy (eV) of the Na^+ ions on the relaxed facets of α-MnO_2 and β-MnO_2.

	Facets	Binding energy per Na^+ ion (eV)
β-MnO_2	{001}	-0.709
	{110}	-0.976
α-MnO_2	{001}	-2.575
	{100}	-1.875

The corresponding charge density difference plots between the absorbed Na^+ ions and facets (**Fig. S11**) show that the larger charge transfer occurred between the absorbed Na^+ ions and the oxygen ligands of β-MnO_2 {001} and {110} facets (**Figs. S11 a and b**) by compared with the Na^+ ions absorbed on the surfaces of α-MnO_2 {001} and {100} facets (**Figs. S11 c - e**). The as-prepared β-MnO_2 nanorods mainly exposed {001} and {110} facets, which could be beneficial for Na^+ ions absorption. Furthermore, together with the moderate binding energy between Na^+

ions and β-MnO_2 {001} and {110} facets, these could result in the better electrochemical performance of the as-prepared β-MnO_2 nanorods compared with α-MnO_2 nanorods.

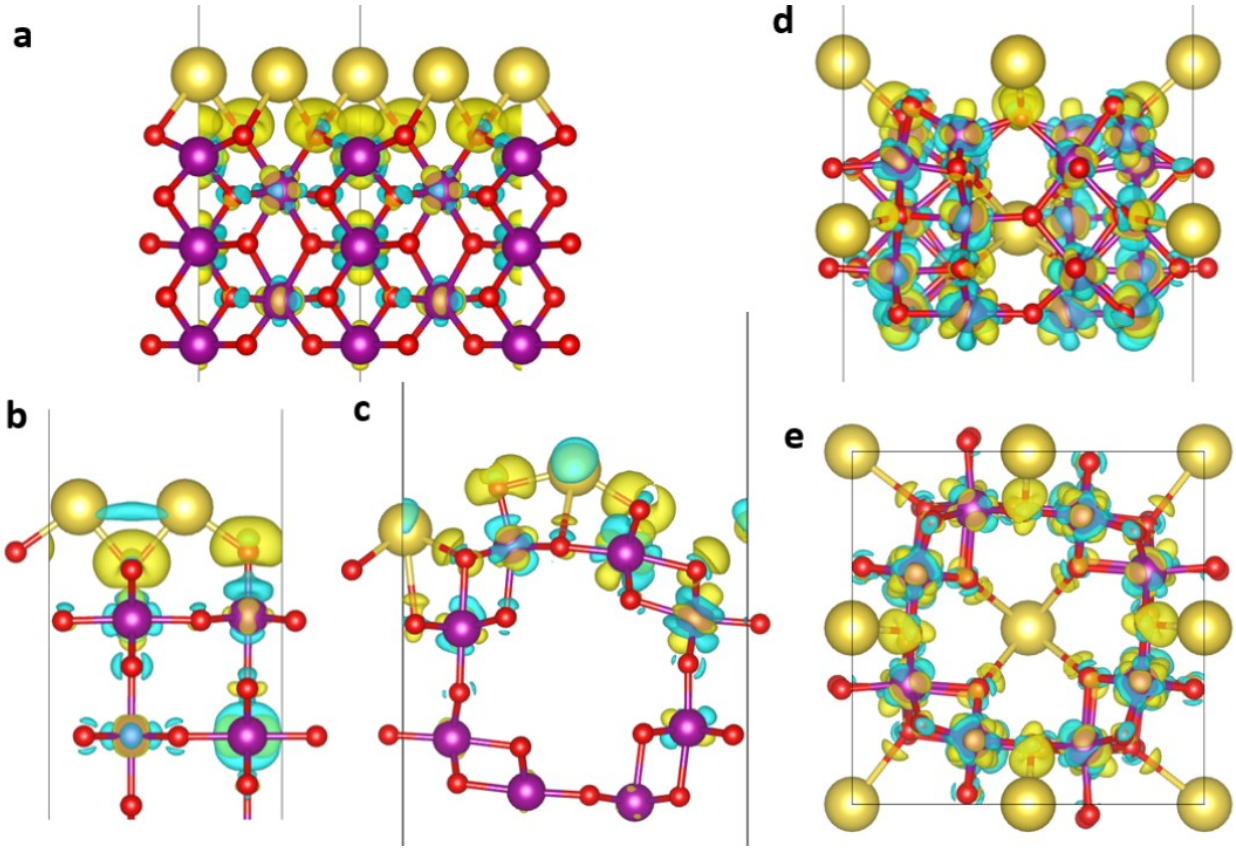

Fig. S11. Charge density difference plots of a. Na^+ ions absorbed {001} facets of β-MnO_2, b. Na^+ ions absorbed {110} facets of β-MnO_2, c. Na^+ ions absorbed {100} facets of α-MnO_2, d and e. side (d) and (top) views of Na^+ ions absorbed {001} facets of α-MnO_2. Electron density isosurface = 0.005 |e|/$Bohr^3$. The coloured regions from turquoise to yellow represent the loss and gain of electrons, respectively. Yellow, purple, and red spheres are Na, Mn, and O atoms, respectively. Plotted by the VESTA.[11]

References:

[1]. G. Kresse, J. Hafner, Ab initio molecular dynamics for liquid metals. ***Phys. Rev. B Condens. Matter,*** 1993, 47, 558–561.

[2]. G. Kresse, J. Hafner, Ab initio molecular-dynamics simulation of the liquid-metal–amorphous-semiconductor transition in germanium. ***Phys. Rev. B Condens. Matter,*** 1994, 49, 14251–14269.

[3]. G. Kresse, J. Furthmüller, Efficiency of ab-initio total energy calculations for metals and semiconductors using a plane-wave basis set. ***Comput. Mater. Sci.*** 1996, 6, 15–50.

[4]. G. Kresse, J. Furthmüller, Efficient iterative schemes for ab initio total-energy calculations using a plane-wave basis set. ***Phys. Rev. B Condens. Matter,*** 1996, 54, 11169–11186.

[5]. J. P. Perdew, M. Ernzerhof, K. Burke, Rationale for mixing exact exchange with density functional approximations. ***J. Chem. Phys***. 1996, 105, 9982–9985.

[6]. Wentao Yao, Gregory M. Odegard, Zhennan Huang, Yifei Yuan, Hasti Asayesh-Ardakani, Soroosh Sharifi-Asl, Meng Cheng, Boao Song, Ramasubramonian Deivanayagam, Fei Long, Craig R. Friedrich, Khalil Amine, Jun Lu, Reza Shahbazian-Yassar, Cations controlled growth of β-MnO_2 crystals with tunable facets for electrochemical energy storage, ***Nano Energy***, 2018, 48, 301-311,

[7]. David A. Tompsett and M. Saiful Islam. Electrochemistry of Hollandite α-MnO_2: Li-Ion and Na-Ion Insertion and Li_2O Incorporation, ***Chem. Mater***. 2013, 25, 2515−252.

[8] S. L. Dudarev, G. A. Botton, S. Y. Savrasov, C. J. Humphreys, A. P. Sutton, Electron-energy-loss spectra and the structural stability of nickel oxide: An LSDA+U study, ***Phys. Rev. B,***

1998, 57, 1505-1509.

[9]. P. E. Blöchl, Projector augmented-wave method. ***Phys. Rev. B Condens. Matter*** 1994, 50, 17953–17979

[10]. H. J. Monkhorst, J. D. Pack, Special points for Brillouin-zone integrations, ***Phys. Rev. B***, 1976, 13, 5188-5192.

[11]. K. Momma and F. Izumi, VESTA 3 for three-dimensional visualization of crystal, volumetric and morphology data, ***J. Appl. Cryst.,*** 2011, 44, 1272–1276,

Beta MnO2 001

1.00000000000000

4.3884270000000001 0.0000000000000000 0.0000000000000000

0.0000000000000000 4.3884270000000001 0.0000000000000000

0.0000000000000000 0.0000000000000000 20.4471980000000002

Mn O Na

5 10 2

Selective dynamics

Direct

0.0000000000000000 0.0000000000000000 0.2445322800000014

0.0000000000000000 0.0000000000000000 0.3744054687925628

0.0000000000000000 0.0000000000000000 0.4941226768596388

0.5000000000000000 0.5000000000000000 0.3027753731473844

0.5000000000000000 0.5000000000000000 0.4491657436820541

0.2953929999999971 0.2953929999999971 0.2445322800000014

0.3021234372914299 0.3021234372914299 0.3788487245889388

0.2740630164519040 0.2740630164519040 0.5223265657878995

0.7046070000000029 0.7046070000000029 0.2445322800000014

0.6978765627085701 0.6978765627085701 0.3788487245889388

0.7259369835480959 0.7259369835480959 0.5223265657878995

0.2013701800265692 0.7986298199734311 0.3079510445056868

0.2142160289306474 0.7857839710693524 0.4413277557056522

0.7986298199734311 0.2013701800265692 0.3079510445056868

0.7857839710693524 0.2142160289306474 0.4413277557056522

0.0000000000000000 0.5000000000000000 0.6024745689906084

0.5000000000000000 0.0000000000000000 0.6024745689906084

Beta MnO2 110

1.00000000000000

2.7235990000000001 0.0000000000000000 0.0000000000000000

0.0000000000000000 6.2061729799999998 0.0000000000000000

0.0000000000000000 0.0000000000000000 23.0394330399999987

Mn O Na

6 12 2

Selective dynamics

Direct

0.5000000000000000 0.8523039999999966 0.2170190000000005

0.5000000000000000 0.3523867070663851 0.3531356073044390

0.5000000000000000 0.8557280926362106 0.4923504306732565

0.0000000000000000 0.3523039999999966 0.2170190000000005

0.0000000000000000 0.8520113392149833 0.3527599347050110

0.0000000000000000 0.3562387867597457 0.4886870757633565

0.5000000000000000 0.8523039999999966 0.2965900000000019

0.5000000000000000 0.3550380395802364 0.4336488102488467

0.5000000000000000 0.8561876075963496 0.5667701818098067

0.5000000000000000 0.3523039999999966 0.2721349999999987

0.5000000000000000 0.8522739109712292 0.4079464807171934

0.5000000000000000 0.3542753583483656 0.5461011256144451

0.0000000000000000 0.0569109999999995 0.2170190000000005

0.0000000000000000 0.5558375284987043 0.3523078478547437

0.0000000000000000 0.0588855011925730 0.4867453638972682

0.0000000000000000 0.6476970000000009 0.2170190000000005

0.0000000000000000 0.1489928945440578 0.3526892893823653

0.0000000000000000 0.6508120271942713 0.4873727958525341

0.5000000000000000 0.1282281011846302 0.6191837401330721

0.5000000000000000 0.5828669547952374 0.6187898638110926

Alpha MnO2 001
1.00000000000000
9.6926000000000005 0.0000000000000000 0.0000000000000000
0.0000000000000000 9.6926000000000005 0.0000000000000000
0.0000000000000000 0.0000000000000000 20.4295009999999984
Na Mn O
4 20 40
Selective dynamics
Direct
0.4999937401634964 0.4999830934473803 0.3603849704025648
-0.0000028353027233 -0.0000082655998679 0.3571968204380189
-0.0000121830869090 0.5000070315986909 0.5849103914802631
0.5000117903321477 -0.0000138154135732 0.5849101070034175
0.3582400000000021 0.1729199999999977 0.2447400000000002
0.3541321129139940 0.1704736332775019 0.3722451343836991
0.3415276940063199 0.1824213641533173 0.4855684249185659
0.6417599999999979 0.8270800000000023 0.2447400000000002
0.6458461063129176 0.8294914890948528 0.3722467300571449
0.6584296977901550 0.8175309577074118 0.4855662063106871
0.8270800000000023 0.3582400000000021 0.2447400000000002
0.8295025428344868 0.3541256718514858 0.3722461170891269
0.8175422649930513 0.3415124050825317 0.4855678260613814
0.1729199999999977 0.6417599999999979 0.2447400000000002
0.1704846145222657 0.6458410251902468 0.3722455800611542
0.1824322059841470 0.6584141492774441 0.4855661667596569
0.8535006974207588 0.6709256999149736 0.3013615889402557
0.8377261823396340 0.6575908636845279 0.4481984819658591
0.1464922948100211 0.3290670239235436 0.3013622581701343
0.1622476921257011 0.3423563852442414 0.4481986723253628
0.3290694139353026 0.8534959353939072 0.3013620600647329
0.3423702585459070 0.8377167922396088 0.4481980819447999
0.6709273917500533 0.1464868975063975 0.3013616224999656
0.6576042222803667 0.1622372660458680 0.4481992346208098
0.1586100000000030 0.1974200000000010 0.2447400000000002
0.1627646941116795 0.2095518146640483 0.3778358529960865
0.1949431063626811 0.2282448586754010 0.5256141157456385
0.8413899999999970 0.8025799999999990 0.2447400000000002
0.8372136515635500 0.7904097140130232 0.3778422360213002
0.8050195841816278 0.7716872548927384 0.5256219380849669

0.8025799999999990	0.1586100000000030	0.2447400000000002
0.7904187580122669	0.1627567218645918	0.3778393176032830
0.7717105745754177	0.1949330811729401	0.5256178433278826
0.1974200000000010	0.8413899999999970	0.2447400000000002
0.2095609951364740	0.8372069518212775	0.3778385582439002
0.2282646742470741	0.8050136926680406	0.5256187400051165
0.6471174957120909	0.6900148430663482	0.3051484525930019
0.6399763055819063	0.6714105754756863	0.4335502587249612
0.3528747253668808	0.3099690819880193	0.3051549579812682
0.3599928831610031	0.3285398011000903	0.4335548493786321
0.3099733642231769	0.6471118584049261	0.3051518576731874
0.3285543900323157	0.6399673105871012	0.4335524151566172
0.6900202402304701	0.3528688925595101	0.3051515386188875
0.6714268912894554	0.3599821965048507	0.4335529868348560
0.5412900000000036	0.1622300000000010	0.2447400000000002
0.5395974815332030	0.1562297431203932	0.3765636843768666
0.5101524342603529	0.1707773829034343	0.5108165510232395
0.4587100000000035	0.8377699999999990	0.2447400000000002
0.4603831176226913	0.8437351606019818	0.3765638053546470
0.4898167299772473	0.8291747282281736	0.5108162720105084
0.8377699999999990	0.5412900000000036	0.2447400000000002
0.8437447837658660	0.5395874622272706	0.3765639367960624
0.8291878246555926	0.5101382159355864	0.5108155444401119
0.1622300000000010	0.4587100000000035	0.2447400000000002
0.1562394398619004	0.4603754807058054	0.3765638439845669
0.1707896445186135	0.4898063379076335	0.5108169242170503
0.0400919044152803	0.6635442938310341	0.3065828938771666
0.0296346517750570	0.6738159178060520	0.4417706941169830
0.9599016961616359	0.3364405524831058	0.3065846016710573
0.9703441558715843	0.3261337989075032	0.4417669720922702
0.3364440468704314	0.0400864960351318	0.3065809642234831
0.3261451679993750	0.0296216144024345	0.4417663727839534
0.6635473408207836	0.9598957169056065	0.3065870242902698
0.6738267739441994	0.9703298591857205	0.4417715051565606

Alpha MnO2 100
1.00000000000000
9.6925530000000002 0.0000000000000000 0.0000000000000000
0.0000000000000000 2.7147589999999999 0.0000000000000000
0.0000000000000000 0.0000000000000000 23.7187809700000010
Mn O Na
8 16 2
Selective dynamics
Direct
0.1729229999999973 0.0000000000000000 0.2992699999999999
0.8289682991491407 0.0000000000000000 0.4170728829934147
0.3528737527735940 0.0000000000000000 0.5063429718816655
0.6417560000000009 0.0000000000000000 0.2235399999999998
0.6824162135030259 0.5000000000000000 0.5146875865780155
0.3270770000000027 0.5000000000000000 0.2108029999999985
0.8582439999999991 0.5000000000000000 0.2865340000000032
0.1523658637980243 0.5000000000000000 0.4286174977528033
0.1974189999999965 0.0000000000000000 0.2176890000000000
0.8187674845575323 0.0000000000000000 0.5000646554339538
0.1477691661904969 0.0000000000000000 0.4864828694106659
0.8413929999999965 0.0000000000000000 0.2335500000000010
0.7010746933930898 0.5000000000000000 0.4305169696143555
0.3025810000000035 0.5000000000000000 0.2923839999999984
0.6586070000000035 0.5000000000000000 0.2765240000000020
0.3386739651594283 0.5000000000000000 0.4516596801362748
0.1717246608347110 0.0000000000000000 0.3752083999025818
0.8359178441633864 0.0000000000000000 0.3411557266344719
0.5429691380007594 0.0000000000000000 0.5142230516133863
0.4587100000000035 0.0000000000000000 0.2191710000000029
0.7227166932169129 0.5000000000000000 0.5838850390988773
0.3121418778079910 0.5000000000000000 0.5579387942720772
0.0412899999999965 0.5000000000000000 0.2909030000000001
0.9640913420644149 0.5000000000000000 0.4225289590781568
0.5029853102324608 0.5000000000000000 0.6056457828557686
0.9936496721229773 0.5000000000000000 0.5342204387148427